In-Vivo Evaluation of a New High Dielectric Constant Material for Local Enhancement of B_1^+ and SNR at 3T

Christopher Sica[1], Sebastian Rupprecht[1], Ray Luo[2], Zhipeng Cao[2], Raffi Sahul[3], Seongtae Kwon[3], Michael Lanagan[4], Christopher Collins[5], and Qing Yang[1,6]

[1]Radiology, Penn State College of Medicine, Hershey, Pennsylvania, United States, [2]Bioengineering, Pennsylvania State University, University Park, Pennsylvania, United States, [3]TRS Technologies Inc, State College, Pennsylvania, United States, [4]Engineering Science and Mechanics, Pennsylvania State University, University Park, Pennsylvania, United States, [5]Radiology, New York University, New York, New York, United States, [6]Neurosurgery, Penn State College of Medicine, Hershey, Pennslyvania, United States

Introduction: Dielectric materials have been utilized in MRI as a mechanism for improving both the transmission efficiency of the RF field and the strength of the reception field. Previous studies have utilized materials with relative permittivity's ranging from 70 to 515 [1-5]. In this work, we evaluate the effects of a new material with a high dielectric constant (~800). This new material is cast in the form of a block, and is monolithic throughout its entire structure. These HDC blocks are evaluated in terms of their effect on B_1^+, SNR, and parallel imaging performance in both a phantom and in-vivo.

Methods: HDC blocks (101mm x 77mm x 14mm) were evaluated with a phantom and an in-vivo brain scan. All data acquisition utilized a 3T Siemens Tim Trio with RF transmission by the volume body coil. Phantom: Seven blocks were placed circumferentially about a large cylindrical phantom. B_1^+ mapping was performed with the AFI technique [6,7], utilizing a 60 degree nominal flip angle and TR1/TR2 of 25/125 ms. A series of 200 low flip angle TurboFLASH images were acquired to perform a multiple repetition SNR measurement. The pixel by pixel SNR was computed as the mean of the 200 measurements at that pixel divided by the corresponding standard deviation. An eight channel head array (In-Vivo Corp) was utilized for reception. Brain: The brain scan utilized seven blocks placed about the back of a volunteer's head, with two additional pads of dielectric constant (~500) placed on top of the forehead. AFI was utilized to acquire flip angle maps, with identical settings to the phantom scan. The TurboFLASH image series acquired 300 images, and this acquisition was repeated three additional times with different undersampling factors enabled (R=2,3,4). The Siemens product reconstruction was utilized to perform the GRAPPA reconstruction. SNR maps were computed for all four cases with the same method as in the phantom (image series mean / image series standard deviation). The SNR maps were also used to calculate geometry factor maps. Geometry factor maps are displayed in relative form, as the geometry factor map with the blocks in place divided by the geometry factor map with no blocks. A twelve channel Siemens head matrix was utilized for reception.

Results: Figure 1 displays an image of the phantom with the blocks in place, along with the acquired normalized B_1^+ map and SNR map. The B_1^+ map demonstrates greater uniformity and efficiency in the region enhanced by the blocks. The SNR maps are roughly equivalent between the two cases in the center of the phantom, and at the edges the scan with blocks possesses up to twice the SNR. The results of the in-vivo brain experiment are displayed in Figure 2. Flip angle maps on the coronal and transverse planes demonstrate interesting behavior – enhancement of the B_1^+ field near the blocks along with a region of uniformity close to the nominal flip angle in the center/middle of the brain. SNR maps at all acceleration factors display improved SNR near the blocks. The SNR within the small ROI's drawn near the back of the head are tabulated in Figure 2, along with the transmission power. Typically 25-40% improvement in SNR is seen at all acceleration factors. The relative geometry factor maps vary from 0.8 to 1.2 at all acceleration factors, indicating the geometry factor map does not change greatly with the addition of the HDC blocks. Transmit power is reduced by 50% in the AFI scan with blocks present.

Discussion: HDC materials possess the ability to strongly reshape the transmit and reception B fields, offering opportunities for local enhancement of B_1^+ and SNR with a reduction of transmission power. The SNR improvement with parallel imaging enabled (R=2,3,4) is less than the fully sampled case (R=1), but this is explained by the relative geometry factor over the ROI, which is about 1.1 to 1.25. Anterior regions of the brain show a relative geometry factor less than 1, indicating parallel imaging will perform better there. The current study represents a work-in-progress, as the HDC material is only available at a fixed permittivity (~800) and form factor (block) at the moment. The ability to alter the form factor and permittivity will lead to more optimal configurations in terms of transmit efficiency, transmit homogeneity, and SNR enhancement. As parallel transmit systems become more common, more control over transmit homogeneity will also be possible on a per-patient basis. The HDC blocks utilized in this study have a low dielectric loss tangent, which leads to increased scan noise. Altering the loss tangent could reduce the scan noise, and raise the SNR improvement numbers even further.

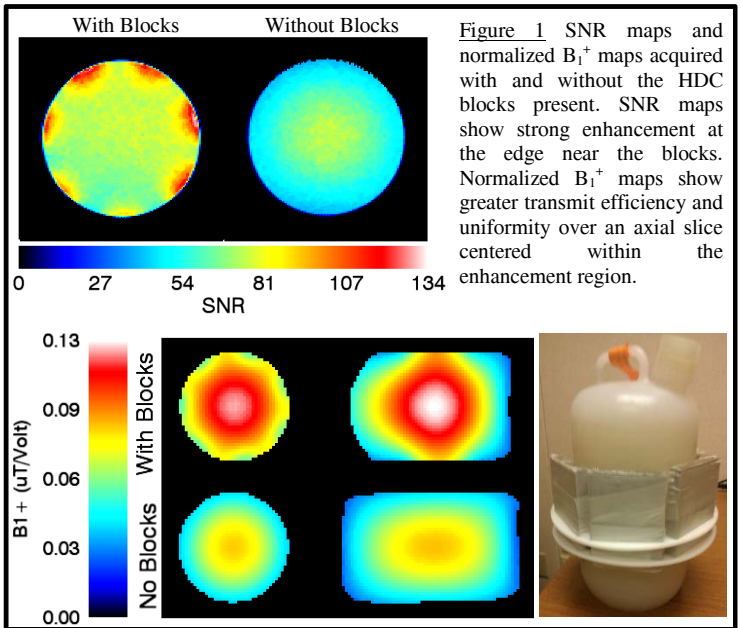

Figure 1 SNR maps and normalized B_1^+ maps acquired with and without the HDC blocks present. SNR maps show strong enhancement at the edge near the blocks. Normalized B_1^+ maps show greater transmit efficiency and uniformity over an axial slice centered within the enhancement region.

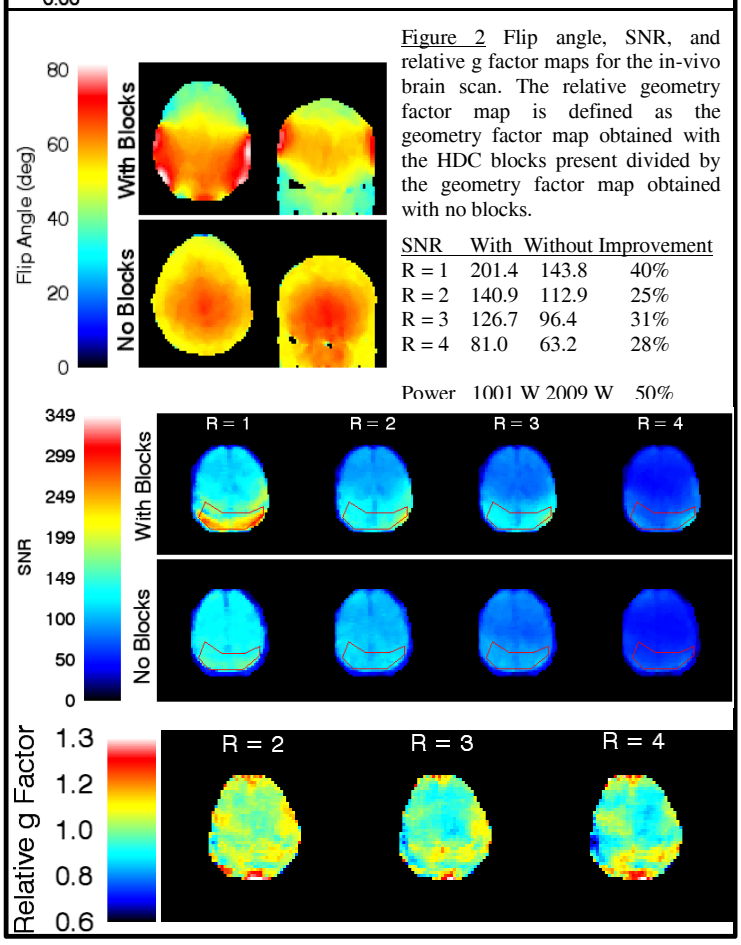

Figure 2 Flip angle, SNR, and relative g factor maps for the in-vivo brain scan. The relative geometry factor map is defined as the geometry factor map obtained with the HDC blocks present divided by the geometry factor map obtained with no blocks.

SNR	With	Without	Improvement
R = 1	201.4	143.8	40%
R = 2	140.9	112.9	25%
R = 3	126.7	96.4	31%
R = 4	81.0	63.2	28%
Power	1001 W	2009 W	50%

References: [1] Yang et al., JMRI 2006. [2] Yang et al., MRM 2010. [3] Teeuwisse et al., MRM 2011. [4] Teeuwisse et al., MRM 2012. [5] Luo et al., MRM 2011. [6] Yarnykh et al., MRM 2007. [7] Nehrke et al., MRM 2009. Acknowledgement: Funding through NIH RO1 EB000454 and The Pennsylvania Department of Health